

2,3-Dipentylidithieno[3,2-*f*:2',3'-*h*]quinoxaline-Based Organic Dyes for Efficient Dye-Sensitized Solar Cells: Effect of π -Bridges and Electron Donors on Solar Cell Performance

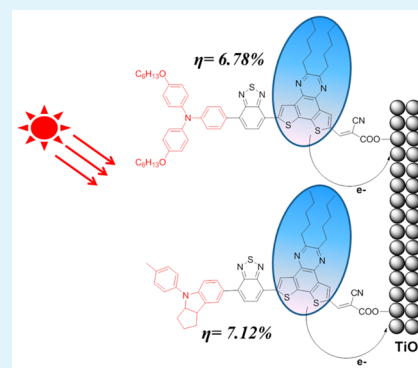
Zu-Sheng Huang,[†] Xu-Feng Zang,[†] Tao Hua,[†] Lingyun Wang,[†] Herbert Meier,[‡] and Derong Cao^{*,†}

[†]School of Chemistry and Chemical Engineering, State Key Laboratory of Luminescent Materials and Devices, South China University of Technology, Guangzhou 510641, China

[‡]Institute of Organic Chemistry, University of Mainz, Mainz 55099, Germany

ABSTRACT: Five novel metal-free organic dyes DQ1–5 containing a dipentylidithieno[3,2-*f*:2',3'-*h*]quinoxaline (DPQ) unit were synthesized and applied in dye-sensitized solar cells (DSSCs), where DPQ was employed as a π -spacer for the first time. Their photophysical, electrochemical, and theoretical calculations and photovoltaic properties were systematically investigated. All the five dyes show broad photoresponse. Especially the absorption edges of DQ3–5 extend to 800 nm on the TiO₂ films. The inserted electron-rich unit 3,4-ethylenedioxythiophene or electron-withdrawing group benzothiadiazole (BTD) in DPQ-based dyes can greatly influence the optoelectronic properties of the dyes. In addition, the different electron donors also significantly affect the performance of the DSSCs. Under standard global AM 1.5 solar light conditions, the DQ5 sensitized solar cell obtained a power conversion efficiency of 7.12%. The result indicates that the rigid DPQ-based organic dye is a promising candidate for efficient DSSCs.

KEYWORDS: metal-free organic dyes, dipentylidithieno[3,2-*f*:2',3'-*h*]quinoxaline, photoresponse, optoelectronic properties, dye-sensitized solar cells



INTRODUCTION

After Grätzel and O'Regan first incorporated the dye-sensitized solar cells (DSSCs) based on the mesoporous TiO₂ films in 1991,¹ enormous attention has been paid to research the DSSCs for their low cost and high photovoltaic performance. Sensitizer, as one of the key components in DSSCs, plays a pivotal role in light-harvesting and electron injection. Among the sensitizers, the ruthenium complexes based devices have achieved high power conversion efficiencies (PCEs), over 11%.^{2–4} Moreover, the DSSCs employing zinc-porphyrin dyes have obtained PCEs up to 13%.^{5–7} However, the high cost and limited availability of ruthenium resources as well as the tedious synthetic procedures and purification difficulty for zinc-porphyrin dyes restrict their further practical application in DSSCs. On the other hand, considerable efforts have been made to develop metal-free organic dyes due to their practical advantages, such as easy structural modification, high molar extinction coefficients, and low cost.^{8–14}

Metal-free organic dyes commonly contain a donor- π -bridge-acceptor (D- π -A) structure and show efficient intramolecular charge transfer (ICT) after photoirradiation. The π -bridge linker between the electron donor and acceptor is of importance in improving the photovoltaic performance of the organic dyes. As we all know, the geometrical configuration of the π -bridge should be relatively planar rather than twisted, which can facilitate the electron transfer from the donor to acceptor. There are some successful molecular designs for high

PCEs by introducing planar moieties into the π -bridges, such as dithieno[3,2-*b*:2',3'-*d*]pyrrole,^{15,16} cyclopentadithiophene,^{17,18} indeno[1,2-*b*]thiophene,^{19,20} naphtho[2,1-*b*:3,4-*b'*]-dithiophene,^{21,22} dithieno[2,3-*d*:2',3'-*d'*]benzo[1,2-*b*:4,5-*b'*]-dithiophene,²³ dithieno[2,3-*d*:2',3'-*d'*]thieno[3,2-*b*:3',2'-*b'*]-dipyrrole,²⁴ and thieno[3,2-*b*][1]benzothiothiophene.²⁵ In our previous studies, we successfully employed a large conjugated planar unit, i.e., dithienopyrrolobenzothiadiazole (DTPBT), which contains a donor-acceptor-donor structure, into the π -bridge and obtained a high efficiency.²⁶ It may indicate that the large planar π -bridge unit with donor-acceptor-donor structure is a promising π -bridge type which can promote the development of metal-free organic dyes.

Actually, dithieno[3,2-*f*:2',3'-*h*]quinoxaline (QDT) is also a donor-acceptor-donor type framework which has been applied in polymer solar cells very recently and behaves with high hole carrier mobility and coplanarity.^{27,28} Based on its unique structural features, QDT may become a promising candidate for the efficient organic dye component. Thus, we intended to use QDT as a basic building block and introduced two pentyl units on it to synthesize the dipentylidithieno[3,2-*f*:2',3'-*h*]quinoxaline (DPQ) moiety. To the best of our

Received: July 15, 2015

Accepted: August 25, 2015

Published: August 25, 2015

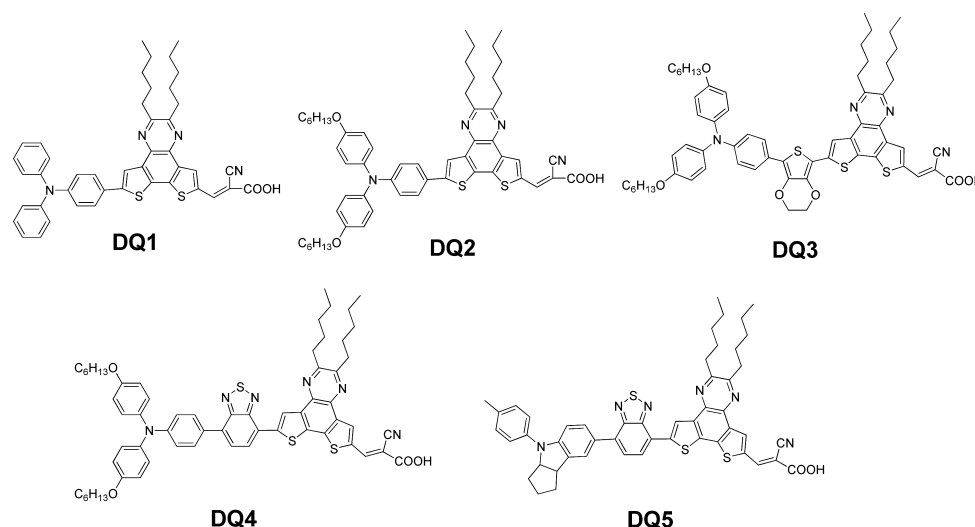


Figure 1. Chemical structures of the dyes **DQ1–5**.

knowledge, there is no report about DPQ-based organic dyes for DSSCs.

In this work, we designed and synthesized five novel metal-free organic dyes (**DQ1–5**) incorporating the DPQ unit as a π -bridge (Figure 1). The design principle was based on the following considerations: first, the introduction of a large planar DPQ unit can effectively delocalize the π -electrons, which can facilitate the ICT of the dyes; second, triphenylamine, dihexyloxy substituted triphenylamine, and indoline were utilized as the electron donors to adjust the HOMO and LUMO energy levels of sensitizers; third, the electron-rich group 3,4-ethylenedioxythiophene (EDOT) or the electron-withdrawing group benzothiadiazole (BTD) was inserted into the π -bridge to extend the absorption spectra, tune the charge transfer property, and narrow the HOMO–LUMO energy gap; fourth, the two alkyl chains on the DPQ and two alkoxy chains on triphenylamine could increase the solubility of dyes, reduce the intermolecular aggregation, and restrict the charge recombination at the TiO_2 surface.^{11,29} The photophysical, electrochemical, and photovoltaic properties of the five sensitizers were systemically investigated.

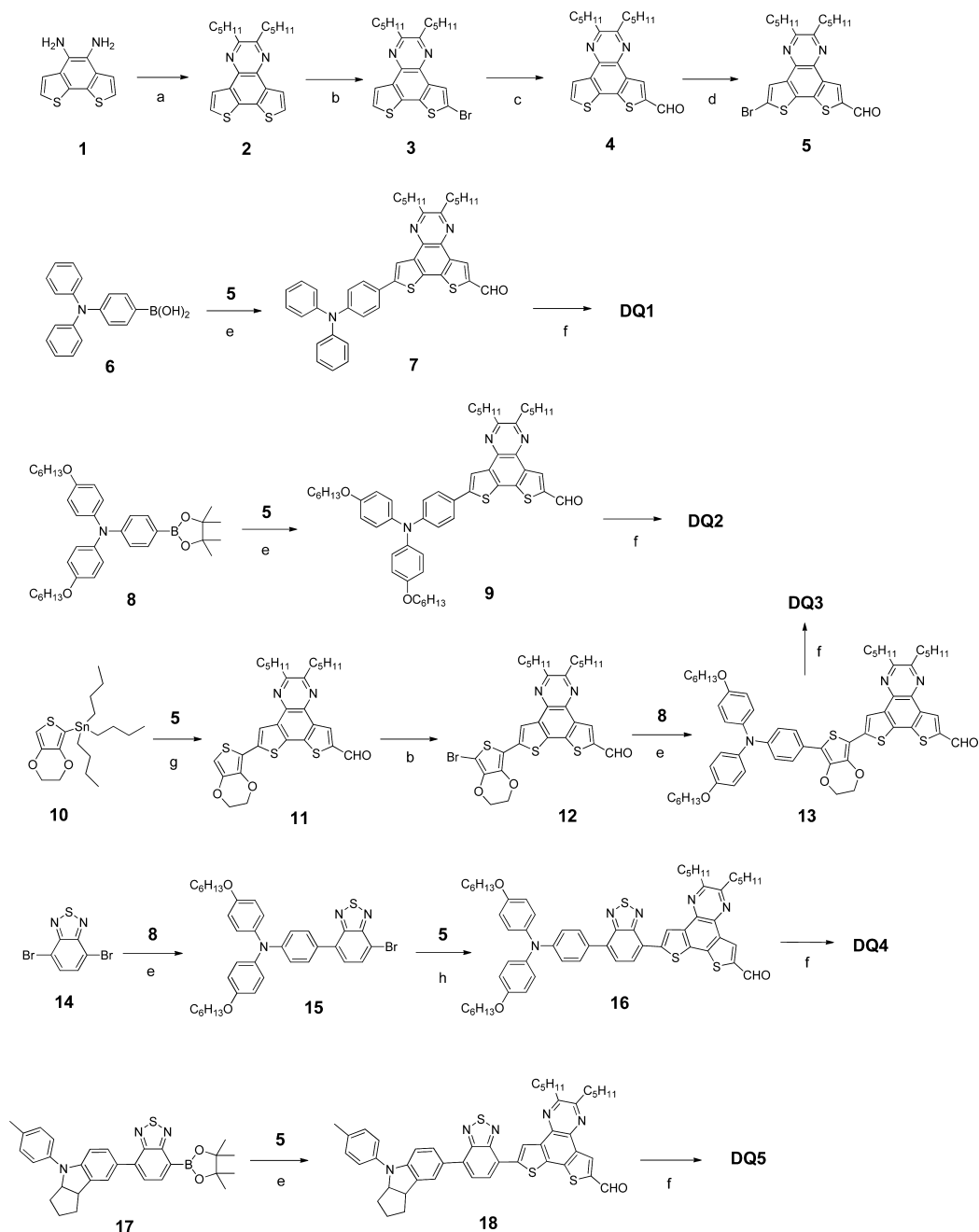
RESULTS AND DISCUSSION

The synthetic route of the dyes **DQ1–5** is presented in Scheme 1. Compounds **1**,³⁰ **8**,³¹ **10**,³² **14**,³³ and **17**³⁴ were synthesized according to the references. The important intermediate **2** was obtained by a cyclization reaction of **1** and dodecane-6,7-dione. Compound **3** was prepared from **2** through bromination with *N*-bromosuccinimide (NBS) and then converted to **4** with *n*-BuLi in dry DMF at -78 °C in a high yield. Compound **5** was synthesized according to another bromination. Aldehydes **7** and **9** were synthesized by the Suzuki–Miyaura reactions. The conventional Knoevenagel condensation reactions of **7** and **9** with *tert*-butyl 2-cyanoacetate produced cyanoacetates. The cyanoacetates were hydrolyzed with trifluoroacetic acid to give target sensitizers **DQ1** and **DQ2**, respectively. **DQ3** was prepared as follows: a Stille coupling reaction of **5** with tributyl(2,3-dihydrothieno[3,4-*b*][1,4]dioxin-5-yl)stannane (**10**) gave **11**. **12** was obtained through a bromination of **11** with NBS in 93% yield. Next, the Suzuki coupling reaction of **12** with borate **8** afforded **13**. Finally, the Knoevenagel condensation reaction of **13** yielded its cyanoacetate derivative,

and then the cyanoacetate was converted into final product **DQ3** in the presence of trifluoroacetic acid. **DQ4** was also prepared from **5** through three Suzuki–Miyaura reactions: a Knoevenagel condensation and a hydrolysis reaction. **DQ5** with the indoline as the electron donor was synthesized from **17** in a similar manner to **DQ2**. All the structures of the intermediates and target sensitizers were fully confirmed by ^1H NMR, ^{13}C NMR, and HRMS.

Photophysical properties. The UV–vis absorption spectra of **DQ1–5** in chloroform (2×10^{-5} M) are depicted in Figure 2a, and the detailed parameters are summarized in Table 1. As shown in Figure 2a, the simplest dye **DQ1** displays the maximum absorption wavelength (λ_{max}) at 496 nm with a molar extinction coefficient (ϵ) of $25450 \text{ M}^{-1} \text{ cm}^{-1}$. The λ_{max} of **DQ2**, **DQ3**, **DQ4**, and **DQ5** are 521 ($\epsilon = 18620 \text{ M}^{-1} \text{ cm}^{-1}$), 553 ($\epsilon = 31850 \text{ M}^{-1} \text{ cm}^{-1}$), 529 ($\epsilon = 29735 \text{ M}^{-1} \text{ cm}^{-1}$), and 547 nm ($\epsilon = 31970 \text{ M}^{-1} \text{ cm}^{-1}$), respectively. **DQ2** shows about 25 nm red-shift of the λ_{max} in comparison with **DQ1**, which is due to increasing the electron donating ability of **DQ2** by incorporation of two alkoxy chains on triphenylamine. After introduction of the electron-withdrawing moiety (BTD) in the π -conjugation system of **DQ2** to form **DQ4**, a bathochromic shift to 529 nm of λ_{max} was observed along with the increase of ϵ to $29735 \text{ M}^{-1} \text{ cm}^{-1}$. Interestingly, when BTD in **DQ2** was replaced with an electron-rich unit (EDOT) to form **DQ3**, a further red-shift of λ_{max} to 553 nm was observed. The bathochromic shifts as well as the increase of the absorption intensity of **DQ3** and **DQ4** in comparison with **DQ2** are attributed to the extended π -conjugation.²² In comparison with **DQ4**, when the donor is changed from dihexyloxy-substituted triphenylamine to indoline, **DQ5** exhibits a redshift of λ_{max} by 18 nm, which may be due to the stronger electron-donating ability of indoline than that of dihexyloxy-substituted triphenylamine. It is found that both **DQ4** and **DQ5** containing BTD show an additional absorption band (around 455 nm) in the visible region, respectively, which indicates that the incorporation of the BTD unit is beneficial to enhance the light-harvesting ability of the dyes.^{34,35}

Time dependent density theory (TD-DFT) calculations were carried out to better understand the excitation energies and transition assignments of the absorption bands of **DQ1–5** (Table 2). According to the calculated results of TD-DFT, the

Scheme 1. Synthetic Routes of DQ1–5ⁱ

ⁱConditions: (a) Dodecane-6,7-dione, acetic acid; (b) NBS, THF; (c) *n*-BuLi, $-78\text{ }^{\circ}\text{C}$, then DMF; (d) NBS, DMF; (e) K_2CO_3 , $\text{Pd}(\text{PPh}_3)_4$, THF; (f) (1) *tert*-butyl 2-cyanoacetate, ammonium acetate, acetic acid, toluene; (2) trifluoroacetic acid; (g) $\text{Pd}(\text{PPh}_3)_2\text{Cl}_2$, THF; (h) (1) 4,4',4'',5,5',5''-octamethyl-2,2'-bi(1,3,2-dioxaborolane), KOAc, $\text{Pd}(\text{dppf})\text{Cl}_2$, dioxane; (2) K_2CO_3 , $\text{Pd}(\text{PPh}_3)_4$, THF.

new absorption bands located at 400–500 nm of **DQ4** and **DQ5** are mainly ascribed to HOMO–1 \rightarrow LUMO (40.3%), HOMO \rightarrow LUMO+1 (49.4%) for **DQ4** and HOMO \rightarrow LUMO+1 (68.6%), and HOMO–1 \rightarrow LUMO (16.7%) for **DQ5**, respectively. The maximum absorptions of **DQ1–5** mainly come from the transition from HOMO to LUMO, and partially from HOMO–1 \rightarrow LUMO and HOMO \rightarrow LUMO +1. In addition, the values of the calculated λ_{max} of the five dyes are similar to the experimental data.

The absorption spectra of **DQ1–5** on TiO_2 films are shown in Figure 2b. A broadening of the spectra can be found when the dyes are adsorbed on the TiO_2 films with respect to those

in the solution, which is favorable to improve light-harvesting and J_{sc} . **DQ1–5** show a λ_{max} at 452, 451, 497, 519, and 519 nm on the TiO_2 films, respectively, with a hypsochromic shift of 44, 70, 56, 10, and 28 nm, respectively, in comparison to those in chloroform solutions. The significant blueshift of the λ_{max} is probably due to the deprotonation of the cyanoacrylic acid group, which weakens the ICT interaction. Such a hypsochromic shift on the TiO_2 films was observed in other organic sensitizers.^{36,37} Obviously, both **DQ4** and **DQ5** with BTB display smaller hypsochromic shifts compared to the other three dyes, which may be attributed to the additional electron-withdrawing group which assists the electron transition process

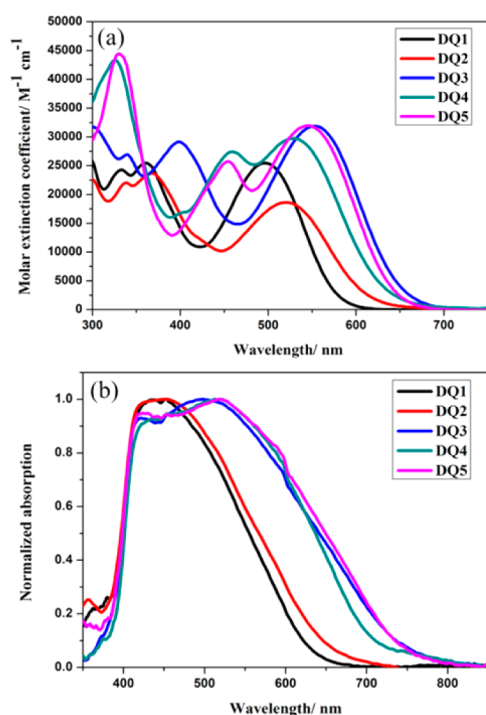


Figure 2. Absorption spectra of DQ1–5 in chloroform solutions (a) and on TiO₂ films (b).

Table 1. Photophysical and Electrochemical Parameters of the Dyes DQ1–5

Dye	λ_{max} (nm) ($\epsilon/M^{-1} \text{cm}^{-1}$) ^a	λ_{max} (nm) on TiO ₂	HOMO (V) (vs NHE) ^b	LUMO (V) (vs NHE) ^c	E_{0-0} (eV) ^d
DQ1	496 (25450)	452	1.22	-0.93	2.15
DQ2	521 (18620)	451	1.00	-1.02	2.02
DQ3	553 (31850)	497	0.88	-1.03	1.91
DQ4	529 (29735)	519	1.07	-0.90	1.97
DQ5	547 (31970)	519	1.00	-0.94	1.94

^aMaximum absorptions of the dyes measured in chloroform with concentration 2×10^{-5} M. ϵ : Molar extinction coefficient at λ_{max} . ^bHOMO of the dyes by cyclic voltammetry in 0.1 M TBAPF₆ in MeCN solutions as supporting electrolyte, Ag/AgCl as the reference electrode, and Pt as counter electrode. Scanning rate: 50 mV s⁻¹. ^cLUMO was calculated by HOMO - E_{0-0} . ^d E_{0-0} was estimated from the onset of the absorption spectrum.

and reduces the effect of deprotonation of cyanoacrylic acid.^{35,38}

Table 2. Calculated TDDFT Excitation Energies (eV), Oscillator Strength (f), and Composition of Excitations with Absorption Wavelengths Longer than 400 nm for Dyes DQ1–5^a

Dye	Wavelength (nm)	E (eV)	Composition ^a	f
DQ1	475.7	2.60	H→L: 84.8%, H-1→L: 10.6%	1.2241
DQ2	502.0	2.47	H→L: 86.2%, H-1→L: 9.5%	1.1924
DQ3	536.4	2.31	H→L: 78.6%, H-1→L: 14.3%	1.6259
	405.8	3.06	H-1→L: 74.1%, H→L: 15.7%	0.1751
DQ4	544.9	2.28	H→L: 71.1%, H-1→L: 12.0%, H→L+1: 13.9%	1.2668
	431.5	2.87	H-1→L: 40.3%, H→L+1: 49.4%	0.4506
DQ5	555.3	2.23	H→L: 74.3%, H→L+1: 15.7%	1.3249
	436.2	2.84	H→L+1: 68.6%, H-1→L: 16.7%	0.2970

^aH = HOMO, L = LUMO, H-1 = HOMO-1, L+1 = LUMO+1.

Electrochemical properties. Cyclic voltammetry was carried out to investigate the electrochemical characteristics of the sensitizers. The cyclic voltammograms are shown in Figure 3, and the relevant electrochemical data are presented in Table

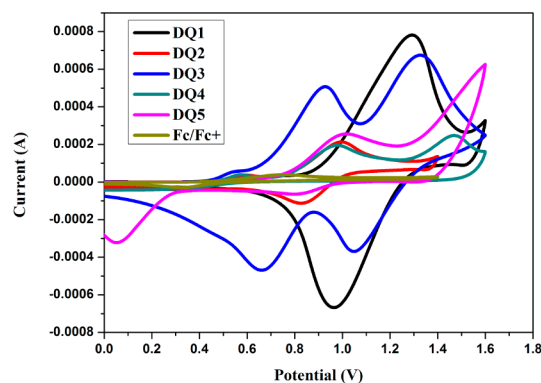
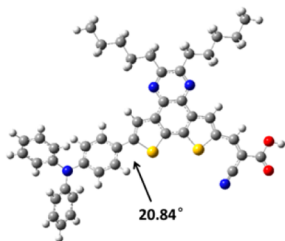
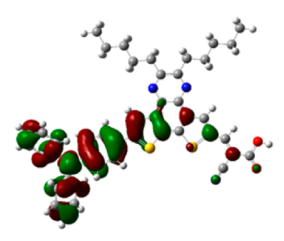
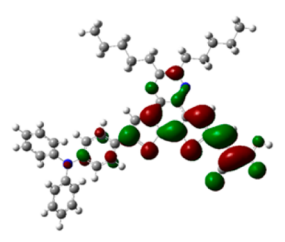
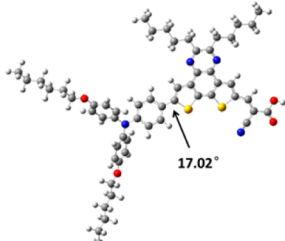
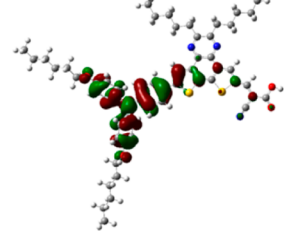
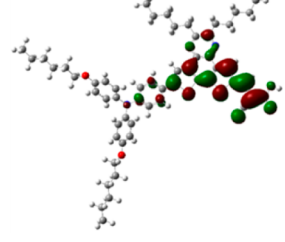
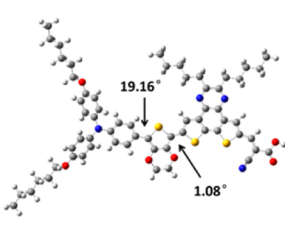
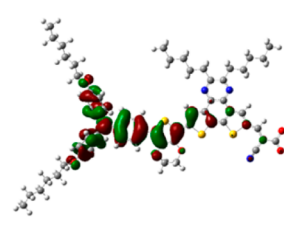
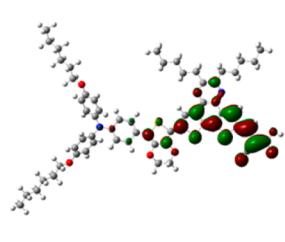
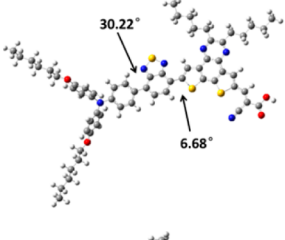
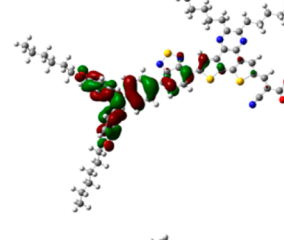
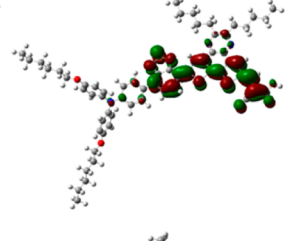
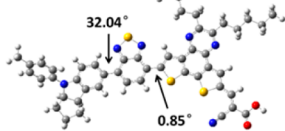
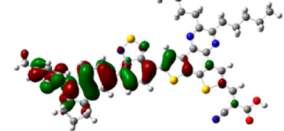
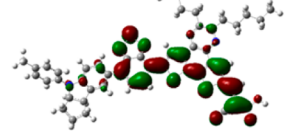


Figure 3. Cyclic voltammograms of DQ1–5.

1. The estimated ground state oxidation potential versus normal hydrogen electrode (vs NHE) corresponds to highest occupied molecular orbital (HOMO) level of the sensitizer. From the view of the data in Table 1, the HOMO levels of DQ1–5 are 1.22, 1.00, 0.88, 1.07, 1.00 V, respectively. Obviously, all the HOMO values are more positive than the redox potential of I^-/I_3^- (0.4 V vs NHE),³⁹ indicating that the oxidized dyes can be regenerated effectively. The band energy gaps (E_{0-0}) of DQ1–5, which are estimated from the onset wavelength of their absorption spectra, are 2.15, 2.02, 1.91, 1.97, and 1.94 eV, respectively. The lowest unoccupied molecular orbital (LUMO) levels of DQ1–5 calculated from HOMO - E_{0-0} are found to be -0.93, -1.02, -1.03, -0.90 and -0.94 V (vs NHE), respectively. As a result, the HOMO levels of these dyes are much negative than the conduction band (CB) of TiO₂ (-0.5 V vs NHE),⁴⁰ demonstrating that the five dyes have sufficient driving force for electron injection from the excited dye to the TiO₂ surface. In comparison with DQ1, when the donor is changed from triphenylamine to dihexyloxy-substituted triphenylamine, DQ2 exhibits a more negative value of HOMO level, which may attribute to the stronger electron-donating ability of dihexyloxy-substituted triphenylamine. In addition, the lifted up HOMO level of DQ5 relative to DQ4 is also due to the stronger electron-donating ability of indoline than that of dihexyloxy-substituted triphenylamine. It should be noted that inserting EDOT or BTD into the spacer part can greatly affect the energy levels of the dyes. The introduction of EDOT into the conjugation promotes the HOMO level of

Table 3. Optimized Structures and Electron Distributions in the HOMO and LUMO Levels of DQ1–5

Dye	Optimized structure	HOMO	LUMO
DQ1			
DQ2			
DQ3			
DQ4			
DQ5			

DQ3 with respect to DQ2. This can be attributed to the increased electron density, which results in a more delocalized HOMO.²² Furthermore, as the electron-withdrawing ability of BTD decreases the electron density of donor, the HOMO level of DQ4 is more positive than that of DQ2. From the view of the data, the embedding of EDOT or BTD can decrease the HOMO–LUMO energy gap. Notably, DQ3 exhibits the highest HOMO level among the five dyes, resulting in smaller difference between the HOMO level of the sensitizer and the redox potential of the I^-/I_3^- couple, leading to slower dye regeneration.⁴¹ As a result, slower dye regeneration would lead to potential back reaction at the TiO_2 /dye/electrolyte interface.

Molecular orbital calculations. In order to investigate the geometrical configuration and electron distributions of the five sensitizers, we performed theoretical calculations based on density functional theory (DFT) with the Gaussian 03W program package at B3LYP/6-31G* level. The optimized

structures and electron distributions of the HOMOs and LUMOs of DQ1–5 are shown in Table 3. With regard to the HOMO states of DQ1–3, the electron density is primarily distributed on the electron donor and nearby linkers. The LUMOs of DQ1–3 localize the electron distribution predominantly on the cyanoacetic acid segment and partly on the DPQ unit. Based on the optimized structures of DQ1–5, the dihedral angle values between the DPQ and nearby units are in the range of 20.84° to 0.68° , leading to an effective conjugation in the π -spacer. The dihedral angles between the donor and BTD in DQ4 and DQ5 are larger than 30° , which is due to the large steric effect between the hydrogen atoms in phenyl and BTD. For the benzothiadiazole-based dyes DQ4 and DQ5, the electron distributions in the HOMOs are largely distributed along the donor-benzothiadiazole system and the LUMOs are mainly concentrated at the benzothiadiazole-DPQ-acceptor system. The well overlapped HOMO and LUMO

orbitals on the benzothiadiazole unit suggest that benzothiadiazole serves as an electron-trap in facilitating the electron transfer from the donor to the acceptor. Similar results were discovered in the pioneering studies.^{42,43} In the optimized structures of the five dyes, the DPQ unit exhibits almost a planar structure.

Adsorption amount. The dye loading amounts of the five dyes on the TiO₂ surface were obtained by desorbing the sensitizers from the films by dipping them into an aqueous solution of NaOH and THF (1:1) for 10 min and measuring the absorbance of the desorbed dye solutions (Table 4).⁴⁴ The

Table 4. Photovoltaic Performance Parameters of the DSSCs Based on DQ1–5

Dye	J_{sc} (mA cm ⁻²)	V_{oc} (mV)	η (%)	FF	Dye loading amount (mol cm ⁻²)
DQ1	13.11	741	6.37	0.65	4.99×10^{-7}
DQ2	9.31	662	4.03	0.65	4.13×10^{-7}
DQ3	9.01	655	4.01	0.68	3.44×10^{-7}
DQ4	14.51	721	6.78	0.65	3.70×10^{-7}
DQ5	17.61	685	7.12	0.59	4.66×10^{-7}

adsorption amounts of DQ1–5 are 4.99×10^{-7} , 4.13×10^{-7} , 3.44×10^{-7} , 3.70×10^{-7} , and 4.66×10^{-7} mol cm⁻², respectively. As we all know, the dye loading amounts are directly related to the molecular size of the dyes.⁴⁵ DQ1 exhibits the highest loading on the TiO₂ film due to its smallest size. DQ3 and DQ4 display lower adsorption amounts than DQ2, which is due to the inserted EDOT and BTM units which increase the molecular configuration.

Photovoltaic performance of the DSSCs. The action spectra of the incident photo-to-current conversion efficiency (IPCE) for the DSSCs with dyes DQ1–5 are shown in Figure 4. All the five dyes can efficiently convert visible light to

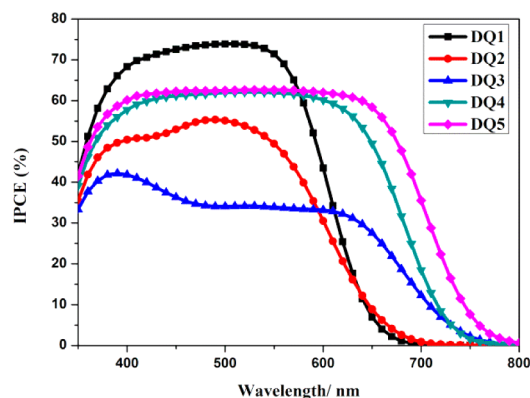


Figure 4. IPCE spectra of the DSSCs based on DQ1–5.

photocurrent in the region from 400 to 700 nm, and DQ3–5 show an even broader spectra response from 400 to 800 nm. The broad spectral ranges are well agreed with the UV–vis absorption on TiO₂ films (Figure 2b). From the view of Figure 4, the IPCE value of DQ5 is over 60% from 400 to 640 nm with a maximum IPCE value of 62.7% at 530 nm, which shows a better IPCE performance than the other four dyes. This result is also in good accordance with the J_{sc} value obtained in J – V (current–voltage) measurements. On the other hand, the IPCE of DQ1, DQ2, DQ3 and DQ4 reach a maximum 73.9% at 500 nm, 55.4% at 490 nm, 42.2% at 390 nm and 62.1% at 530 nm,

respectively. By extending π -conjugation length with BTM, the IPCE performance of DQ4 is impressively improved with broader photoresponse coverage and much higher value in comparison with that of DQ2. Although DQ3 extends the IPCE response than DQ2 via embedding EDOT, the IPCE value of DQ3 is much lower than that of DQ2. As mentioned previously, the upshift of the HOMO energy level of DQ3 leads to its slower driving force for dye regeneration, which is also contributed to its low charge collection efficiency in the DSSCs.^{41,46} By changing the donor from triphenylamine (DQ1) to dihexyloxy-substituted triphenylamine (DQ2), the photoresponse cannot be effectively broadened. However, a broader IPCE spectrum of DQ5 can be found when the donor dihexyloxy-substituted triphenylamine of DQ4 is changed to indoline.

The solar-to-electricity conversion efficiencies of the DSSCs sensitized by DQ1–5 were evaluated by measuring the J – V characteristics at 100 mW cm⁻² simulated AM 1.5G solar light without mask (Figure 5). The detailed photovoltaic parameters

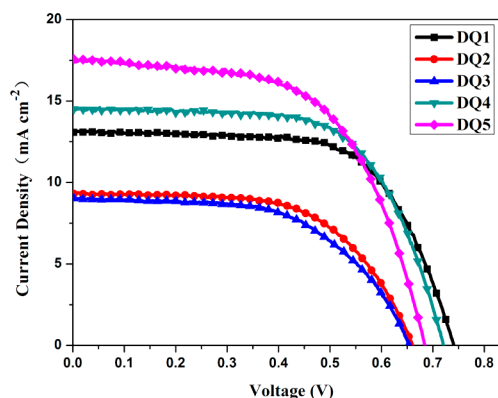


Figure 5. J – V curves of the DSSCs based on DQ1–5.

of short-circuit photocurrent (J_{sc}), open-circuit photovoltage (V_{oc}), fill factor (FF) and power conversion efficiency (η) are summarized in Table 4. The device sensitized by DQ5 shows the best overall conversion efficiency of 7.12% with a J_{sc} of 17.61 mA cm⁻², a V_{oc} of 685 mV, and an FF of 0.59. The DSSCs based on DQ1–4 obtain efficiencies of 6.37%, 4.03%, 4.01% and 6.78%, respectively. In particular, the DSSC based on DQ5 presents the highest η due to its highest J_{sc} . The large J_{sc} of DQ5 can be ascribed to a high molar extinction coefficient, broad absorption spectra and appropriate HOMO and LUMO levels. This result agrees well with the corresponding IPCE spectra. DQ3 displays poor performance with low J_{sc} and V_{oc} , even though it has a high molar extinction coefficient and broad absorption response. It might be speculated that the upshift of HOMO level of DQ3 results in less efficient regeneration of the oxidized dye after electron injection due to the diminished gap between the HOMO and the potential of the redox couple. Moreover, the low V_{oc} of DQ3 may result from the apparently charge recombination (vide infra). DQ1 exhibits much higher η value than DQ2 because it has higher molar extinction coefficient, larger adsorption amount, larger driving force of oxidized dye regeneration and much higher V_{oc} . The DSSC sensitized by DQ4 shows much better performance than DQ2 due to the inserted electron-withdrawing unit BTM which significantly broadens and strengthens the absorption and increases the electron lifetime.

CDCA (chenodeoxycholic acid) has been verified that it can prevent the aggregation of dyes on TiO₂ surface, and then improve the performance of the DSSCs.⁴⁷ Therefore, in order to study the intermolecular interactions of the dyes on the TiO₂ surface, the effect of coadsorbent CDCA on the performance of the DSSCs were investigated (Figure 6, Table 5). Upon

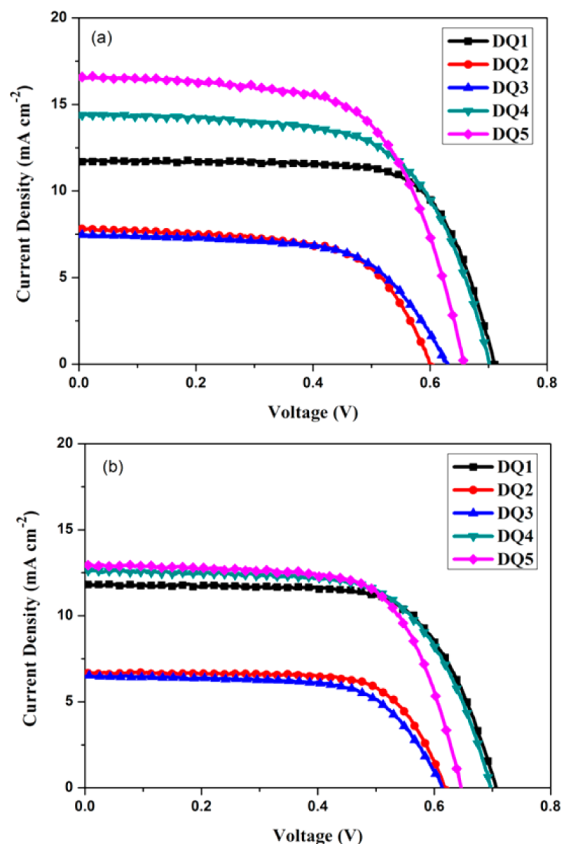


Figure 6. J - V curves of the DSSCs based on DQ1-5 with 1 mM CDCA (a) and with 10 mM CDCA (b).

Table 5. Photovoltaic Performance Parameters of the DSSCs Based on DQ1-5 with CDCA

Dye	CDCA	J_{sc} (mA cm ⁻²)	V_{oc} (mV)	η (%)	FF
DQ1	0 mM	13.11	741	6.37	0.65
	1 mM	11.75	710	6.00	0.72
	10 mM	11.71	707	5.75	0.69
DQ2	0 mM	9.31	662	4.03	0.65
	1 mM	7.83	601	3.49	0.74
	10 mM	6.68	619	2.94	0.71
DQ3	0 mM	9.01	655	4.01	0.68
	1 mM	7.47	631	3.50	0.74
	10 mM	6.46	615	2.66	0.67
DQ4	0 mM	14.51	721	6.78	0.65
	1 mM	14.28	702	6.45	0.64
	10 mM	12.63	698	5.80	0.66
DQ5	0 mM	17.61	685	7.12	0.59
	1 mM	16.47	658	6.94	0.64
	10 mM	12.89	648	5.71	0.68

coadsorption of CDCA, the J_{sc} of the five dyes decreased, resulting in a decrease of the η values. A possible explanation is that there is no or less aggregation of dyes on TiO₂ surface, but the adsorption amount of the dye on the TiO₂ surface is

reduced by the coadsorption of CDCA, resulting in a loss of active light-harvesting.⁴⁸ This result suggests that DQ1-5 can already effectively suppress dye aggregation of the π -conjugation backbone and inhibit intermolecular interactions on the TiO₂ films.

In order to further understand the correlation between the charge transfer process and the photovoltaic properties of the DSSCs, electrochemical impedance spectroscopy (EIS) was carried out in the dark. The Nyquist plots for the DSSCs based on DQ1-5 are displayed in Figure 7a. The smaller semicircle at

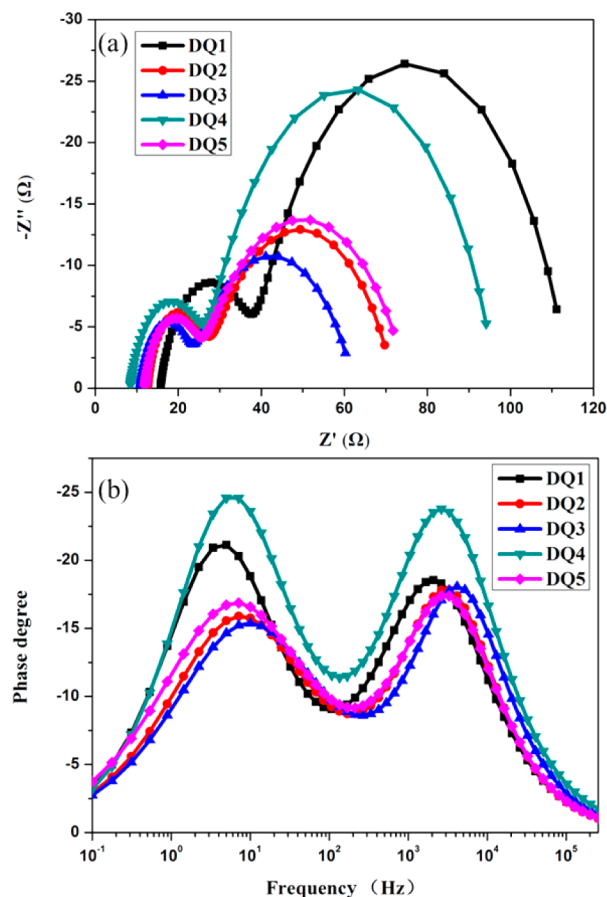


Figure 7. Electrochemical impedance spectra of the DSSCs based on DQ1-5 measured in the dark: (a) Nyquist plots; (b) bode phase plots.

higher frequencies corresponds to the charge transfer at the Pt/electrolyte interface, while the larger semicircle at the lower frequencies accords to the charge transfer at the TiO₂/dye/electrolyte interface.^{49,50} The charge recombination resistance (R_{rec}) at the TiO₂ surface can be deduced by fitting curves using Z-view software. The R_{rec} values of DQ1-5 decrease in the order of DQ1 (76 Ω) > DQ4 (70 Ω) > DQ5 (51 Ω) > DQ2 (46 Ω) > DQ3 (40 Ω). A smaller R_{rec} indicates a faster charge recombination and a larger dark current.⁵¹ Hence, DQ1 and DQ4 possess more effective suppression of the recombination of injection electron with I₃⁻ in the electrolyte than the other three dyes. Because the narrowest gap between HOMO level and the redox potential of the I⁻/I₃⁻ couple, the reduction rate of the excited DQ3 is low, causing serious electron recombination. The trend of the R_{rec} appears to be consistent with the decrease order of V_{oc} . In the Bode phase plots (Figure 7b), the peak of the middle frequency is related to

the electron lifetime, and a lower frequency of the peak corresponds to a longer electron lifetime. The value of the middle frequency peak decreases in the order of **DQ3** > **DQ2** > **DQ5** > **DQ4** > **DQ1**. The electron lifetime (τ_n) can be estimated from $\tau_n = 1/(2\pi f_p)$, where f_p is the peak frequency in lower frequency.⁵⁸ Thus, the electron lifetime of the five dyes decreases in the order of **DQ1** (36.4 ms) > **DQ4** (27.6 ms) > **DQ5** (23.1 ms) > **DQ2** (21.0 ms) > **DQ3** (15.9 ms). These data further support the order of the V_{oc} of the DSSCs based on **DQ1**–**5**.

CONCLUSION

In summary, we developed five novel metal-free organic dyes **DQ1**–**5** with a DPQ unit as a π -spacer. The results show that DPQ is a novel promising π -spacer unit. These dyes exhibit a broad photospectral response. Especially **DQ3**–**5** extend the absorption edges to 800 nm on the TiO₂ films. The DPQ-based organic dyes have well coplanar geometry and show effective electron separation from HOMO levels to LUMO levels, which is confirmed by DFT and TDDFT calculations. The different donors greatly influence the performance of the dyes. For **DQ1** and **DQ2**, triphenylamine as the electron-donor brings better photovoltaic performance compared with dihexyloxy substituted triphenylamine. For the benzothiadiazole-based dyes **DQ4** and **DQ5**, indoline as the donor shows better performance than dihexyloxy substituted triphenylamine. Moreover, it is found that the incorporation of the electron-rich unit EDOT or the electron-withdrawing unit BTD can significantly broaden the photoresponse, narrow the HOMO–LUMO energy gap, and obviously affect the photovoltaic performance of the dyes. By contrast with the reference dye (**DQ2**), introduction of EDOT into the π -bridge of **DQ3** greatly upshifts the HOMO energy level and decreases the electron lifetime. In addition, incorporation of BTD causes better electron transition properties, larger IPCE value, and more effective suppression of electron recombination. Finally, **DQ5** with indoline as donor and BTD as additional π -bridge yields the highest conversion efficiency of 7.12% under standard global AM 1.5G solar light illumination conditions.

EXPERIMENTAL SECTION

Materials and instruments. All reagents were purchased from J&K Chemical Ltd., Adamas and Aladdin in analytical grade without any further purification. The organic solvents were carefully dried and distilled according to standard process. All reactions were carried out under argon atmosphere and monitored by thin-layer chromatography. Flash chromatography separations were performed on silica gel of 300–400 mesh.

¹H and ¹³C NMR spectra were recorded on a Burkert 400 MHz instrument with CDCl₃ and THF-*d*₈. Melting points were measured on a SGW X-4B microscopic melting point apparatus. High resolution electrospray ionization mass spectrometry (HR ESI-MS) analyses were performed on an Agilent Technologies 1290 Infinity mass spectrophotometer. Ultraviolet–visible (UV–vis) spectra of the organic dyes in the solution were measured on a Shimadzu UV-2450 spectrophotometer. The UV–vis absorption spectra of the sensitizers adsorbed on TiO₂ films were recorded on a Shimadzu UV-3010 spectrophotometer. The dye adsorption amount on TiO₂ films were obtained by desorbing the dyes from TiO₂ surface with 0.1 M NaOH in THF/H₂O (*v/v* = 1:1) and measured the UV–vis spectra of the solution. Cyclic voltammetry (CV) was carried out on an electrochemistry workstation (e-corder (ED 401) potentiostat) using a three electrode cell at room temperature with a scan rate of 50 mV s⁻¹. The dye sensitized photoanode was used as the working electrode, a platinum wire as the counter electrode and Ag/AgCl (3 M in KCl) as a

reference electrode. The solution of tetrabutylammoniumhexafluorophosphate (TBAPF₆) (0.1 M) in dry acetonitrile was applied as supporting electrolyte. The ferrocene/ferrocenium (Fc/Fc⁺) redox couple used for potential calibration. The electrochemical redox potentials of sensitizers versus NHE were calibrated by addition of 0.63 V to the potentials versus (Fc/Fc⁺). The incident monochromatic photo-to-current conversion efficiency (IPCE) spectra were measured on a PEC-S20 action spectrum measurement system. The photo-current–voltage characteristics were carried out on a Keithley 2400 source meter under simulated AM 1.5G (100 mW cm⁻²) illumination with a standard solar light simulator (Pecell-L15, Japan) without a mask. The electrochemical impedance spectroscopy (EIS) measurements were recorded on Zahner Zennium electrochemical workstation in the dark under a forward bias of –0.80 V with a frequency range of 0.1 Hz to 100 kHz.

Computational details. The vertical excitation energies were calculated by TDDFT at MPW1K/6-31G** levels.⁵² We selected chloroform to consider the solvent effect. The solvent effect was simulated by the conductor-like polarizable continuum model (C-PCM).¹⁸ All the calculations were carried out with the Gaussian 09 program package.

Synthesis of dyes. *2,3-Dipentylidithieno[3,2-f:2',3'-h]-quinoxaline (2)*. A solution of **1** (1.70 g, 7.73 mmol) and dodecane-6,7-dione (1.61 g, 8.12 mmol) in acetic acid (20 mL) was stirred under argon atmosphere at 100 °C for 24 h. After cooling to room temperature, the reaction was quenched by water. The mixture was extracted with CH₂Cl₂. The combined organic layer was washed with water and dried over anhydrous MgSO₄. After removal of the solvent under reduced pressure, the residue was purified by column chromatography on silica gel with ethyl acetate/petroleum ether (*v/v* = 1/10) as the eluent. **2** was obtained as a cream-colored solid in 51% yield (1.5 g), mp 62–64 °C. ¹H NMR (400 MHz, CDCl₃) δ 8.27–8.26 (m, 2H), 7.50–7.48 (m, 2H), 3.04 (t, *J* = 7.6 Hz, 4H), 1.97–1.90 (m, 4H), 1.51–1.48 (m, 8H), 0.99 (t, *J* = 6.4 Hz, 6H). ¹³C NMR (100 MHz, CDCl₃) δ 154.3, 154.3, 136.2, 135.1, 133.9, 124.1, 34.9, 31.9, 28.1, 22.7, 14.1. HRMS (ESI, *m/z*): [M + H]⁺ calcd for C₂₂H₂₇N₂S₂: 383.1610, found: 383.1610.

6-Bromo-2,3-dipentylidithieno[3,2-f:2',3'-h]quinoxaline (3). To a solution of **2** (672 mg, 2 mmol) in THF (20 mL), NBS (427 mg, 2.4 mmol) was added slowly at 0 °C. The reaction mixture was stirred for 12 h, and quenched by water. The mixture was extracted with CH₂Cl₂ three times, and the combined organic layer was washed with brine and dried over anhydrous MgSO₄. After evaporation of the solvent under reduced pressure, the residue was purified by column chromatography on silica gel with ethyl acetate/petroleum ether (*v/v* = 1/40) as the eluent. **3** was obtained as cream-colored solid in 86% yield (791 mg), mp 65–67 °C. ¹H NMR (400 MHz, CDCl₃) δ 8.19 (d, *J* = 5.2 Hz, 1H), 8.15 (s, 1H), 7.46 (d, *J* = 5.2 Hz, 1H), 3.03–2.97 (m, 4H), 1.95–1.86 (m, 4H), 1.47–1.41 (m, 8H), 0.99–0.96 (m, 6H). ¹³C NMR (100 MHz, CDCl₃) δ 154.8, 154.6, 135.9, 135.2, 134.9, 134.8, 134.7, 132.6, 126.7, 124.4, 124.0, 112.4, 34.9, 31.9, 28.0, 28.0, 22.7, 14.1. HRMS (ESI, *m/z*): [M + H]⁺ calcd for C₂₂H₂₆⁷⁹BrN₂S₂: 461.0715, found: 461.0716; [M + H]⁺ calcd for C₂₂H₂₆⁸¹BrN₂S₂: 463.0695, found: 463.0703.

2,3-Dipentylidithieno[3,2-f:2',3'-h]quinoxaline-6-carbaldehyde (4). To a solution of **3** (1.02 g, 2.22 mmol) in dry THF (20 mL), 2.4 M *n*-BuLi in hexane solution (1.11 mL, 2.66 mmol) was added dropwise under argon atmosphere. After the reaction mixture was stirred at –78 °C for 2 h, DMF (0.21 mL, 2.66 mmol) was added in one portion. After warming up to room temperature within 5 h, the mixture was poured into aqueous NH₄Cl solution. The mixture was extracted with CH₂Cl₂, and the combined organic layer was washed with brine and dried over anhydrous MgSO₄. The solvent was removed under reduced vacuum and the residue was purified by column chromatography on silica gel with ethyl acetate/petroleum ether (*v/v* = 1/30) as the eluent. **4** was obtained as a faint yellow solid in 46% (419 mg), mp 70–72 °C. ¹H NMR (400 MHz, CDCl₃) δ 10.18 (s, 1H), 8.92 (s, 1H), 8.30 (d, *J* = 5.2 Hz, 1H), 7.67 (d, *J* = 5.2 Hz, 1H), 3.07 (t, *J* = 7.7 Hz, 4H), 1.97–1.90 (m, 4H), 1.53–1.40 (m, 8H), 0.96 (t, *J* = 6.7 Hz, 6H). ¹³C NMR (100 MHz, CDCl₃) δ 183.8,

155.5, 155.3, 141.4, 138.8, 138.1, 136.5, 136.4, 134.5, 133.9, 133.2, 127.1, 124.4, 35.0, 34.9, 31.9, 31.8, 28.1, 28.0, 22.6, 14.1, 14.1. HRMS (ESI, m/z): $[M + H]^+$ calcd for $C_{23}H_{27}N_2OS_2$: 411.1559, found: 411.1555.

9-Bromo-2,3-dipentylidithieno[3,2-f:2',3'-h]quinoxaline-6-carbaldehyde (5). To a solution of **4** (300 mg, 0.73 mmol) in DMF (20 mL), NBS (196 mg, 1.1 mmol) was added in one portion and the reaction mixture was stirred at 70 °C for 12 h. After cooling to room temperature, the mixture was poured into water, and extracted with CH_2Cl_2 . The combined organic phase was washed with water three times and dried over anhydrous $MgSO_4$. After removal of the solvent under reduced pressure, the residue was purified by column chromatography on silica gel with ethyl acetate/petroleum ether ($v/v = 1/30$) as the eluent. **5** was obtained as a faint yellow solid in 85% (303 mg), mp 124–126 °C. 1H NMR (400 MHz, $CDCl_3$) δ 10.17 (s, 1H), 8.89 (s, 1H), 8.26 (s, 1H), 3.08–3.03 (m, 4H), 1.96–1.88 (m, 4H), 1.48–1.40 (m, 8H), 0.96 (t, $J = 6.7$ Hz, 6H). ^{13}C NMR (100 MHz, $CDCl_3$) δ 183.6, 155.7, 155.7, 141.6, 137.7, 137.0, 136.2, 135.0, 134.5, 133.8, 133.5, 127.0, 115.8, 35.0, 34.9, 31.9, 27.9, 27.8, 22.6, 14.1. HRMS (ESI, m/z): $[M + H]^+$ calcd for $C_{23}H_{26}^{79}BrN_2OS_2$: 489.0664, found: 489.0660; $[M + H]^+$ calcd for $C_{23}H_{26}^{81}BrN_2OS_2$: 491.0645, found: 491.0638.

9-(4-(Diphenylamino)phenyl)-2,3-dipentylidithieno[3,2-f:2',3'-h]quinoxaline-6-carbaldehyde (7). To a mixture of **5** (129 mg, 0.264 mmol), (4-(diphenylamino)phenyl)boronic acid (**6**) (115 mg, 0.40 mmol), K_2CO_3 aqueous solution (2 M, 0.4 mL) and THF (15 mL), $Pd(PPh_3)_4$ (30 mg, 0.026 mmol) was added. The reaction mixture was stirred for 16 h under argon atmosphere at 70 °C. After cooling to room temperature, the mixture was quenched by water, and extracted with CH_2Cl_2 three times. The combined organic phase was washed with brine then dried over anhydrous $MgSO_4$. After removal of the solvent under reduced pressure, the residue was purified by column chromatography on silica gel with ethyl acetate/dichloromethane/petroleum ether ($v/v/v = 1/5/30$) as the eluent. **7** was obtained as an orange-yellow solid in 63% yield (108 mg), mp 229–231 °C. 1H NMR (400 MHz, $CDCl_3$) δ 10.14 (s, 1H), 8.87 (s, 1H), 8.34 (s, 1H), 7.67 (m, 2H), 7.33–7.29 (m, 4H), 7.18–7.07 (m, 8H), 3.07–3.04 (m, 4H), 1.94–1.87 (m, 4H), 1.47 (m, 8H), 0.98–0.96 (m, 6H). ^{13}C NMR (100 MHz, $CDCl_3$) δ 183.8, 155.5, 155.3, 148.5, 147.2, 146.1, 141.1, 139.3, 138.7, 136.8, 136.2, 134.3, 134.1, 131.8, 129.5, 127.4, 127.0, 125.0, 123.7, 122.9, 118.4, 35.0, 31.9, 28.2, 28.2, 22.6, 14.1. HRMS (ESI, m/z): $[M + H]^+$ calcd for $C_{41}H_{40}N_3OS_2$: 654.2607, found: 654.2605.

9-(4-(Bis(4-(hexyloxy)phenyl)amino)phenyl)-2,3-dipentylidithieno[3,2-f:2',3'-h]quinoxaline-6-carbaldehyde (9). The synthesis procedure for **9** was similar to that of **7**, except 4-(hexyloxy)-*N*-(4-(hexyloxy)phenyl)-*N*-(4-(4,4,5,5-tetramethyl-1,3,2-dioxaborolan-2-yl)phenyl)aniline (**8**) instead of (4-(diphenylamino)phenyl)boronic acid (**6**). **9** was obtained as a yellow solid in 72% yield (125 mg), mp 55–57 °C. 1H NMR (400 MHz, $CDCl_3$) δ 10.15 (s, 1H), 8.89 (s, 1H), 8.30 (s, 1H), 7.60 (d, $J = 8.4$ Hz, 2H), 7.11 (d, $J = 8.6$ Hz, 4H), 6.97 (d, $J = 8.4$ Hz, 2H), 6.86 (d, $J = 8.6$ Hz, 4H), 3.96 (t, $J = 6.4$ Hz, 4H), 3.06 (t, $J = 7.4$ Hz, 4H), 1.96–1.89 (m, 4H), 1.83–1.76 (m, 4H), 1.48–1.43 (m, 12H), 1.36–1.35 (m, 8H), 0.98–0.91 (m, 12H). ^{13}C NMR (100 MHz, $CDCl_3$) δ 183.5, 156.0, 155.1, 154.9, 149.4, 146.3, 140.8, 140.0, 139.1, 138.3, 136.4, 135.8, 133.9, 133.8, 131.0, 127.1, 127.1, 124.9, 119.6, 117.4, 115.5, 68.3, 34.9, 32.0, 31.7, 29.4, 27.9, 27.9, 25.8, 22.7, 22.7, 14.2, 14.1. HRMS (ESI, m/z): $[M + H]^+$ calcd for $C_{53}H_{64}N_3O_3S_2$: 854.4384, found: 854.4383.

9-(2,3-Dihydrothieno[3,4-b][1,4]dioxin-5-yl)-2,3-dipentylidithieno[3,2-f:2',3'-h]quinoxaline-6-carbaldehyde (11). To a solution of tributyl(2,3-dihydrothieno[3,4-b][1,4]dioxin-5-yl)stannane (**10**) (216 mg, 0.50 mmol) and **5** (189 mg, 0.387 mmol) in THF (20 mL), $Pd(PPh_3)_2Cl_2$ (27 mg, 0.039 mmol) was added. The reaction mixture was stirred under argon for 20 h at 75 °C. After cooling to room temperature, the mixture was poured into water and extracted with CH_2Cl_2 three times. The combined organic solution was washed with brine and dried over anhydrous $MgSO_4$. After the solvent was evaporated under reduced pressure, the crude product was purified by column chromatography with ethyl acetate/dichloromethane/petroleum ether ($v/v/v = 1/1/10$) as the eluent. **11** was obtained as a

yellow solid in 87% yield (185 mg), mp 170–172 °C. 1H NMR (400 MHz, $CDCl_3$) δ 10.16 (s, 1H), 8.90 (s, 1H), 8.28 (s, 1H), 6.40 (s, 1H), 4.48–4.47 (m, 2H), 4.33 (m, 2H), 3.08–3.05 (m, 4H), 1.95–1.89 (m, 4H), 1.48 (m, 8H), 0.98–0.97 (m, 6H). ^{13}C NMR (100 MHz, $CDCl_3$) δ 183.8, 155.4, 155.3, 142.0, 141.1, 139.3, 138.6, 138.1, 138.1, 136.8, 136.7, 136.0, 134.1, 131.7, 118.2, 111.8, 99.3, 65.3, 64.6, 35.0, 31.9, 28.2, 28.1, 22.7, 14.1. HRMS (ESI, m/z): $[M + H]^+$ calcd for $C_{29}H_{31}N_2O_3S_3$: 551.1491, found: 551.1490.

9-(7-(Bromo-2,3-dihydrothieno[3,4-b][1,4]dioxin-5-yl)-2,3-dipentylidithieno[3,2-f:2',3'-h]quinoxaline-6-carbaldehyde (12). The reaction was carried out in a similar manner as **3**. The crude product was purified on a silica gel column with ethyl acetate/dichloromethane/petroleum ether ($v/v/v = 1/1/10$) as the eluent. **12** was obtained as a yellow solid in 93% yield, mp 200–202 °C. 1H NMR (400 MHz, $CDCl_3$) δ 10.04 (s, 1H), 8.66 (s, 1H), 7.87 (s, 1H), 4.44–4.39 (m, 4H), 2.96 (t, $J = 7.4$ Hz, 4H), 1.90–1.88 (m, 4H), 1.48 (m, 8H), 0.99–0.98 (m, 6H). ^{13}C NMR (100 MHz, $CDCl_3$) δ 183.8, 155.5, 155.5, 141.2, 140.4, 138.4, 138.4, 138.1, 136.8, 136.0, 135.6, 134.4, 134.1, 131.9, 118.4, 112.0, 87.7, 65.3, 65.0, 35.0, 31.9, 28.2, 28.1, 22.6, 14.1. HRMS (ESI, m/z): $[M + H]^+$ calcd for $C_{29}H_{30}^{79}BrN_2O_3S_3$: 629.0596, found: 629.0598; $[M + H]^+$ calcd for $C_{29}H_{30}^{81}BrN_2O_3S_3$: 631.0578, found: 631.0555.

9-(7-(4-(Bis(4-(hexyloxy)phenyl)amino)phenyl)-2,3-dihydrothieno[3,4-b][1,4]dioxin-5-yl)-2,3-dipentylidithieno[3,2-f:2',3'-h]quinoxaline-6-carbaldehyde (13). The synthetic procedure for **13** was similar to that of **9**. **13** was obtained as a viscous liquid in 68% yield. 1H NMR (400 MHz, $CDCl_3$) δ 10.08 (s, 1H), 8.77 (s, 1H), 8.09 (s, 1H), 7.55 (m, 2H), 7.07 (m, 4H), 6.93 (m, 2H), 6.84 (m, 4H), 4.47–4.37 (m, 4H), 3.94 (t, $J = 5.4$ Hz, 4H), 3.01 (m, 4H), 1.92 (m, 4H), 1.80–1.77 (m, 4H), 1.48 (m, 12H), 1.36 (m, 8H), 0.99–0.92 (m, 12H). ^{13}C NMR (100 MHz, $CDCl_3$) δ 183.8, 155.8, 155.3, 155.2, 148.0, 140.9, 140.5, 139.9, 138.7, 138.4, 137.2, 137.0, 136.8, 136.0, 134.2, 134.0, 131.5, 127.0, 126.9, 124.4, 120.3, 118.1, 117.6, 115.5, 108.4, 68.4, 65.3, 64.8, 35.1, 35.1, 32.1, 31.8, 29.8, 29.5, 28.3, 28.2, 25.9, 22.8, 22.8, 14.3, 14.2. HRMS (ESI, m/z): $[M + H]^+$ calcd for $C_{59}H_{68}N_3O_5S_3$: 994.4316, found: 994.4323.

4-(7-Bromobenzo[*c*][1,2,5]thiadiazol-4-yl)-*N,N*-bis(4-(hexyloxy)phenyl)aniline (15). To a mixture of **8** (1.55 g, 2.72 mmol), 4,7-dibromobenzo[*c*][1,2,5]thiadiazole (**14**) (0.96 g, 3.26 mmol), K_2CO_3 aqueous solution (2 M, 4 mL) and THF (25 mL), $Pd(PPh_3)_4$ (156 mg, 0.136 mmol) was added as a catalyst. The reaction mixture was stirred for 10 h under argon at 70 °C. After cooling to room temperature, water was added to quench the reaction. The mixture was then extracted with CH_2Cl_2 three times and the combined organic solution was washed with brine then dried over anhydrous $MgSO_4$. The solvent was removed under reduced pressure, and the crude product was purified by silica gel column chromatography with dichloromethane/petroleum ether ($v/v = 3/1$) as the eluent. **15** was obtained as red oil in 61% yield (1.09 g). 1H NMR (400 MHz, $CDCl_3$) δ 7.83 (d, $J = 7.4$ Hz, 1H), 7.74 (m, 2H), 7.47 (d, $J = 7.4$ Hz, 1H), 7.12 (m, 4H), 7.03 (m, 2H), 6.86 (m, 4H), 3.95 (t, $J = 6.1$ Hz, 4H), 1.81–1.76 (m, 4H), 1.48 (m, 4H), 1.36 (m, 8H), 0.93 (m, 6H). ^{13}C NMR (100 MHz, $CDCl_3$) δ 155.9, 154.0, 153.2, 149.4, 140.2, 133.8, 132.4, 129.8, 127.7, 127.2, 126.8, 119.4, 115.4, 111.6, 68.3, 31.7, 29.4, 25.8, 22.7, 14.1. HRMS (ESI, m/z): $[M + H]^+$ calcd for $C_{36}H_{41}^{79}BrN_3O_2S$: 658.2097, found: 658.2091; $[M + H]^+$ calcd for $C_{36}H_{41}^{81}BrN_3O_2S$: 660.2083, found: 660.2079.

9-(7-(4-(Bis(4-(hexyloxy)phenyl)amino)phenyl)benzo[*c*][1,2,5]thiadiazol-4-yl)-2,3-dipentylidithieno[3,2-f:2',3'-h]quinoxaline-6-carbaldehyde (16). To a mixture of **15** (452 mg, 0.69 mmol), bis(pinacolato)diboron (876 mg, 3.45 mmol), potassium acetate (338 mg, 3.45 mmol) in 1,4-dioxane (20 mL), $Pd(dppf)Cl_2$ (51.8 mg, 0.069 mmol) was added. The reaction mixture was stirred under argon atmosphere at 100 °C for 24 h. After cooling to room temperature, the solvent was evaporated under reduced pressure and the residue was purified by column chromatography on a silica gel column (dichloromethane/petroleum ether, $v/v = 2/1$) to give a red liquid. The resulting red liquid was mixed with **5** (168.7 mg, 0.345 mmol), K_2CO_3 aqueous solution (2 M, 0.5 mL), $Pd(PPh_3)_4$ (40 mg, 0.035 mmol) and THF (15 mL). Then the reaction was carried out in a

similar manner as 7. The crude product was chromatographed on a silica gel column with dichloromethane/petroleum ether ($v/v = 1/1$) as the eluent. **16** was obtained as a red solid in 19% yield for the two reaction steps (129 mg), mp 72–74 °C. ^1H NMR (400 MHz, CDCl_3) δ 10.09 (s, 1H), 9.00 (s, 1H), 8.77 (s, 1H), 8.02 (m, 1H), 7.82 (m, 2H), 7.63 (m, 1H), 7.13 (m, 4H), 7.04 (m, 2H), 6.87 (m, 4H), 3.96 (t, $J = 6.4$ Hz, 4H), 3.08–3.00 (m, 4H), 2.01–1.88 (m, 4H), 1.83–1.76 (m, 4H), 1.57–1.43 (m, 12H), 1.36 (m, 8H), 1.03–0.91 (m, 12H). ^{13}C NMR (100 MHz, CDCl_3) δ 183.5, 155.9, 155.3, 155.07, 153.6, 152.5, 149.3, 141.3, 140.8, 140.1, 138.2, 136.4, 136.1, 134.5, 133.7, 133.5, 133.3, 129.8, 127.9, 127.2, 126.7, 126.0, 123.9, 122.5, 119.3, 115.4, 68.3, 34.9, 32.0, 32.0, 31.6, 30.9, 29.4, 28.1, 27.9, 25.8, 22.8, 22.7, 22.6, 14.2, 14.1. HRMS (ESI, m/z): $[\text{M} + \text{Na}]^+$ calcd for $\text{C}_{59}\text{H}_{65}\text{N}_5\text{NaO}_3\text{S}_3$: 1010.4142, found: 1010.4144.

2,3-Dipentyl-9-(7-(4-(*p*-tolyl)-1,2,3,3a,4,8b-hexahydrocyclopenta[b]indol-7-yl)benzo[c][1,2,5]thiadiazol-4-yl)dithieno[3,2-*f*:2',3'-*h*]quinoxaline-6-carbaldehyde (18). To a mixture of **17** (292 mg, 0.573 mmol), **5** (140 mg, 0.286 mmol), K_2CO_3 aqueous solution (2 M, 0.43 mL) and THF (15 mL), $\text{Pd}(\text{PPh}_3)_4$ (33 mg, 0.029 mmol) was added as a catalyst. The reaction mixture was stirred under argon at 70 °C for 18 h, and quenched by water. The mixture was extracted with CH_2Cl_2 three times, and the combined organic layer was dried over anhydrous MgSO_4 . After removal of the solvent, the residue was purified by gel silica column chromatography (dichloromethane/petroleum ether, $v/v = 1/1$) to give a purple solid with a yield of 54% (122 mg), mp 136–138 °C. ^1H NMR (400 MHz, CDCl_3) δ 10.12 (s, 1H), 9.05 (s, 1H), 8.82 (s, 1H), 8.06 (m, 1H), 7.80 (s, 1H), 7.75 (m, 1H), 7.66 (m, 1H), 7.26–7.17 (m, 4H), 7.02 (m, 1H), 4.89–4.86 (m, 1H), 3.96–3.91 (t, $J = 8.2$ Hz, 1H), 3.11–3.03 (m, 4H), 2.36 (s, 3H), 2.12–1.67 (m, 10H), 1.53–1.41 (m, 8H), 1.03–0.96 (m, 6H). ^{13}C NMR (100 MHz, CDCl_3) δ 183.7, 155.4, 155.1, 153.8, 152.7, 148.7, 141.3, 141.1, 140.1, 138.3, 136.5, 136.2, 135.5, 134.6, 134.3, 133.9, 133.3, 131.9, 131.1, 123.0, 129.2, 129.2, 129.0, 126.9, 126.8, 125.6, 125.5, 123.4, 122.4, 120.5, 107.5, 69.4, 65.7, 45.5, 35.4, 35.1, 33.8, 32.1, 30.7, 29.8, 28.2, 28.1, 24.6, 22.9, 22.8, 21.0, 19.3, 14.4, 14.3. HRMS (ESI, m/z): $[\text{M} + \text{Na}]^+$ calcd for $\text{C}_{47}\text{H}_{45}\text{N}_5\text{NaO}_3\text{S}_3$: 814.2678, found: 814.2672.

(*E*)-2-Cyano-3-(9-(4-(*diphenylamino*)phenyl)-2,3-dipentyl)dithieno[3,2-*f*:2',3'-*h*]quinoxalin-6-yl)acrylic acid (DQ1). A mixture of **7** (110 mg, 0.168 mmol), *tert*-butyl 2-cyanoacetate (71.1 mg, 0.504 mmol), ammonium acetate (38.8 mg, 0.504 mmol) and acetic acid (2 mL) in toluene (20 mL) was stirred at 130 °C under argon atmosphere for 3 h. After cooling to room temperature, the mixture was poured into water and extracted with CH_2Cl_2 . The organic layer was dried over anhydrous MgSO_4 and the solvent was evaporated by reduced pressure. The crude product was purified by silica gel column chromatography (ethyl acetate/dichloromethane/petroleum ether, $v/v/v = 1/5/30$) to give a red solid. The resulting solid was dissolved in trifluoroacetic acid (10 mL), and stirred for 4 h at room temperature. The reaction mixture was poured into water (10 mL), and the resulting crude red solid was collected through filtration and washed with water (200 mL) three times to give **DQ1** as red solid, mp 252–254 °C. The yield for the two steps was 71% (86 mg). ^1H NMR (400 MHz, $\text{THF}-d_8$) δ 8.64 (s, 1H), 8.53 (s, 1H), 8.26 (s, 1H), 7.70 (m, 2H), 7.32–7.28 (m, 4H), 7.17–7.05 (m, 8H), 3.04–3.01 (m, 4H), 1.95 (m, 4H), 1.48 (m, 8H), 0.97 (t, $J = 6.1$ Hz, 6H). ^{13}C NMR (100 MHz, $\text{THF}-d_8$) δ 163.8, 156.2, 156.0, 149.6, 148.3, 147.3, 146.9, 140.1, 138.7, 136.9, 136.8, 136.3, 135.2, 134.6, 131.7, 130.3, 128.1, 127.9, 125.9, 124.5, 123.6, 119.1, 116.3, 101.6, 35.7, 35.6, 32.9, 28.7, 28.5, 23.6, 23.6, 14.5. HRMS (ESI, m/z): $[\text{M} + \text{Na}]^+$ calcd for $\text{C}_{44}\text{H}_{40}\text{N}_4\text{NaO}_2\text{S}_2$: 743.2485, found: 743.2505.

(*E*)-3-(9-(4-(*Bis*(4-(*hexyloxy*)phenyl)amino)phenyl)-2,3-dipentyl)dithieno[3,2-*f*:2',3'-*h*]quinoxalin-6-yl)-2-cyanoacrylic acid (DQ2). **DQ2** was synthesized from **9** by the same procedure as that of **DQ1**. **DQ2** was obtained as a black solid in 68% yield, mp 248–250 °C. ^1H NMR (400 MHz, $\text{THF}-d_8$) δ 8.83 (s, 1H), 8.62 (s, 1H), 8.32 (s, 1H), 7.65 (m, 2H), 7.09 (m, 4H), 6.95 (m, 2H), 6.88 (m, 4H), 3.96 (t, $J = 6.3$ Hz, 4H), 3.10–3.07 (m, 4H), 2.01–1.92 (m, 4H), 1.81–1.76 (m, 4H), 1.50–1.43 (m, 12H), 1.38–1.37 (m, 8H), 0.98–0.91 (m, 12H). ^{13}C NMR (101 MHz, $\text{THF}-d_8$) δ 163.8, 157.3, 156.1, 155.9, 150.6, 147.6, 147.3, 140.9, 140.2, 138.9, 137.0, 136.8, 136.3, 135.0,

134.4, 131.4, 128.0, 127.9, 125.7, 120.3, 118.2, 116.4, 116.1, 101.4, 68.8, 35.6, 35.6, 32.9, 32.8, 32.6, 30.3, 28.7, 28.5, 26.7, 23.6, 23.5, 23.5, 14.5, 14.4. HRMS (ESI, m/z): $[\text{M} + \text{Na}]^+$ calcd for $\text{C}_{56}\text{H}_{64}\text{N}_4\text{NaO}_4\text{S}_2$: 943.4261, found: 943.4261.

(*E*)-3-(9-(7-(4-(*Bis*(4-(*hexyloxy*)phenyl)amino)phenyl)-2,3-dihydrothieno[3,4-*b*][1,4]dioxin-5-yl)-2,3-dipentyl)dithieno[3,2-*f*:2',3'-*h*]quinoxalin-6-yl)-2-cyanoacrylic acid (DQ3). The synthesis method of **DQ3** from **13** was similar to that of **DQ1**. **DQ3** was obtained as a black solid in 72% yield, mp 220–222 °C. ^1H NMR (400 MHz, $\text{THF}-d_8$) δ 8.55 (s, 1H), 8.48 (s, 1H), 7.91 (s, 1H), 7.56 (m, 2H), 7.04 (d, $J = 8.5$ Hz, 4H), 6.90–6.84 (m, 6H), 4.50–4.39 (m, 4H), 3.95 (t, $J = 6.3$ Hz, 4H), 3.02–2.95 (m, 4H), 1.95–1.92 (m, 4H), 1.81–1.76 (m, 4H), 1.50–1.48 (m, 12H), 1.37 (m, 8H), 1.02–0.92 (m, 12H). ^{13}C NMR (100 MHz, $\text{THF}-d_8$) δ 163.9, 156.9, 155.9, 155.7, 148.8, 147.3, 141.4, 141.3, 138.9, 138.7, 138.4, 137.9, 136.8, 136.4, 134.7, 134.2, 131.4, 127.6, 127.5, 125.4, 120.8, 118.5, 117.5, 116.5, 116.0, 108.7, 100.9, 68.8, 66.2, 65.6, 35.6, 35.6, 32.9, 32.9, 32.6, 30.3, 28.6, 28.3, 26.8, 23.6, 23.5, 14.6, 14.6, 14.4. HRMS (ESI, m/z): $[\text{M} + \text{Na}]^+$ calcd for $\text{C}_{62}\text{H}_{68}\text{N}_4\text{NaO}_6\text{S}_3$: 1083.4193, found: 1083.4205.

(*E*)-3-(9-(7-(4-(*Bis*(4-(*hexyloxy*)phenyl)amino)phenyl)benzo[c][1,2,5]thiadiazol-4-yl)-2,3-dipentyl)dithieno[3,2-*f*:2',3'-*h*]quinoxalin-6-yl)-2-cyanoacrylic acid (DQ4). The synthesis method of **DQ4** from **16** was similar to that of **DQ1**. **DQ4** was obtained as a black solid in 75% yield, mp 265–267 °C. ^1H NMR (400 MHz, $\text{THF}-d_8$) δ 8.46 (s, 1H), 8.24 (s, 1H), 8.16 (s, 1H), 7.74 (m, 2H), 7.68 (m, 1H), 7.38 (m, 1H), 7.07 (m, 4H), 6.93 (m, 2H), 6.87 (m, 4H), 3.96 (t, $J = 5.7$ Hz, 4H), 2.89–2.87 (m, 2H), 2.78–2.77 (m, 2H), 1.93 (m, 2H), 1.80–1.78 (m, 6H), 1.53 (m, 8H), 1.39 (m, 12H), 1.04 (m, 3H), 0.95 (m, 9H). ^{13}C NMR (100 MHz, $\text{THF}-d_8$) δ 163.9, 157.0, 155.7, 155.3, 154.1, 153.0, 149.9, 147.1, 141.5, 141.2, 138.6, 138.3, 136.4, 136.3, 136.1, 134.9, 134.4, 133.7, 133.3, 130.7, 128.9, 128.0, 127.0, 126.5, 124.2, 122.7, 119.8, 116.3, 116.1, 101.0, 68.8, 35.5, 33.0, 33.0, 32.6, 30.4, 28.3, 27.9, 26.8, 23.7, 23.7, 23.6, 14.8, 14.7, 14.4. HRMS (ESI, m/z): $[\text{M} + \text{H}]^+$ calcd for $\text{C}_{62}\text{H}_{67}\text{N}_6\text{O}_4\text{S}_3$: 1055.4380, found: 1055.4398.

(*E*)-2-Cyano-3-(2,3-dipentyl-9-(7-(4-(*p*-tolyl)-1,2,3,3a,4,8b-hexahydrocyclopenta[b]indol-7-yl)benzo[c][1,2,5]thiadiazol-4-yl)dithieno[3,2-*f*:2',3'-*h*]quinoxalin-6-yl)acrylic acid (DQ5). The synthesis method of **DQ5** from **18** was similar to that of **DQ1**. **DQ5** was obtained as a black solid in 70% yield, mp 220–222 °C. ^1H NMR (400 MHz, $\text{THF}-d_8$) δ 8.58 (s, 1H), 8.31 (s, 1H), 8.28 (s, 1H), 7.77 (s, 1H), 7.73–7.66 (m, 2H), 7.41 (m, 1H), 7.22–7.21 (m, 2H), 7.15–7.13 (m, 2H), 6.90 (m, 1H), 4.84 (m, 1H), 3.83 (t, $J = 8.1$ Hz, 1H), 2.96–2.83 (m, 4H), 2.32 (s, 3H), 1.95–1.83 (m, 6H), 1.55–1.42 (m, 12H), 1.05–0.97 (m, 6H). ^{13}C NMR (100 MHz, $\text{THF}-d_8$) δ 163.8, 155.8, 155.4, 154.2, 153.2, 149.1, 147.2, 141.9, 141.2, 138.8, 138.4, 136.6, 136.4, 136.1, 135.9, 135.0, 134.5, 134.5, 133.2, 132.0, 130.5, 130.0, 127.9, 127.3, 126.4, 125.9, 123.7, 122.7, 120.9, 116.3, 108.0, 101.0, 70.0, 46.3, 36.1, 35.6, 35.5, 34.5, 33.0, 33.0, 28.4, 28.0, 23.7, 23.7, 20.9, 14.7, 14.6. HRMS (ESI, m/z): $[\text{M} + \text{Na}]^+$ calcd for $\text{C}_{50}\text{H}_{46}\text{N}_6\text{NaO}_2\text{S}_3$: 881.2737, found: 881.2752.

Fabrication of dye-sensitized solar cells. The TiO_2 films (~ 12 μm in thickness) with a scattering layer (~ 4 μm) were prepared according to a previous procedure.⁴⁶ The TiO_2 photoanodes were immersed in a solution of dyes for 16 h in the dark (0.3 mM dye in chloroform). After adsorption of the dyes, the films were washed with chloroform and dried. The dye-sensitized TiO_2 /FTO glass films together with the Pt/FTO counter electrode were assembled into sandwiched type solar cells. The electrolyte (0.6 M 1-methyl-3-propylimidazolium iodide (PMII), 0.1 M guanidinium thiocyanate, 0.07 M I_2 , 0.05 M LiI, and 0.5 M *tert*-butylpyridine in acetonitrile/valeronitrile (85:15)) was injected from a hole made on the counter electrode into the space between the sandwiched cells. The active area of the dye coated TiO_2 was 0.16 cm^2 .

AUTHOR INFORMATION

Corresponding Author

* Tel./fax: +86 20 87110245. E-mail: drcao@scut.edu.cn (D. Cao).

Notes

The authors declare no competing financial interest.

ACKNOWLEDGMENTS

We are grateful to the National Natural Science Foundation of China (21272079), the Science and Technology Planning Project of Guangdong Province, China (2013B010405003), and the Fundamental Research Funds for the Central Universities (2014ZP0008).

REFERENCES

- (1) O'Regan, B.; Grätzel, M. A Low-Cost, High-Efficiency Solar Cell Based on Dye-Sensitized Colloidal TiO₂ Films. *Nature* **1991**, *353*, 737–740.
- (2) Wu, W. Q.; Xu, Y. F.; Rao, H. S.; Su, C. Y.; Kuang, D. B. Multistack Integration of Three-Dimensional Hyperbranched Anatase Titania Architectures for High-Efficiency Dye-Sensitized Solar Cells. *J. Am. Chem. Soc.* **2014**, *136*, 6437–6445.
- (3) Nazeeruddin, M. K.; Pechy, P.; Renouard, T.; Zakeeruddin, S. M.; Humphry-Baker, R.; Comte, P.; Liska, P.; Cevey, L.; Costa, E.; Shklover, V.; Spiccia, L.; Deacon, G. B.; Bignozzi, C. A.; Grätzel, M. Engineering of Efficient Panchromatic Sensitizers for Nanocrystalline TiO₂-Based Solar Cells. *J. Am. Chem. Soc.* **2001**, *123*, 1613–1624.
- (4) Chen, C.-Y.; Wang, M.; Li, J.-Y.; Pootrakulchote, N.; Alibabaei, L.; Ngoc-le, C.-h.; Decoppet, J.-D.; Tsai, J.-H.; Grätzel, C.; Wu, C.-G.; Zakeeruddin, S. M.; Grätzel, M. Highly Efficient Light-Harvesting Ruthenium Sensitizer for Thin-Film Dye-Sensitized Solar Cells. *ACS Nano* **2009**, *3*, 3103–3109.
- (5) Yella, A.; Mai, C. L.; Zakeeruddin, S. M.; Chang, S. N.; Hsieh, C. H.; Yeh, C. Y.; Grätzel, M. Molecular Engineering of Push-Pull Porphyrin Dyes for Highly Efficient Dye-Sensitized Solar Cells: the Role of Benzene Spacers. *Angew. Chem., Int. Ed.* **2014**, *53*, 2973–2977.
- (6) Mathew, S.; Yella, A.; Gao, P.; Humphry-Baker, R.; Curchod, B. F. E.; Ashari-Astani, N.; Tavernelli, I.; Rothlisberger, U.; Nazeeruddin, M. K.; Grätzel, M. Dye-Sensitized Solar Cells with 13% Efficiency Achieved Through the Molecular Engineering of Porphyrin Sensitizers. *Nat. Chem.* **2014**, *6*, 242–247.
- (7) Luo, J.; Xu, M.; Li, R.; Huang, K. W.; Jiang, C.; Qi, Q.; Zeng, W.; Zhang, J.; Chi, C.; Wang, P.; Wu, J. N-Annulated Perylene as an Efficient Electron Donor for Porphyrin-Based Dyes: Enhanced Light-Harvesting Ability and High-Efficiency Co(II/III)-Based Dye-Sensitized Solar Cells. *J. Am. Chem. Soc.* **2014**, *136*, 265–272.
- (8) Yang, J.; Ganesan, P.; Teuscher, J.; Moehl, T.; Kim, Y. J.; Yi, C.; Comte, P.; Pei, K.; Holcombe, T. W.; Nazeeruddin, M. K.; Hua, J.; Zakeeruddin, S. M.; Tian, H.; Grätzel, M. Influence of the Donor Size in D- π -A Organic Dyes for Dye-Sensitized Solar Cells. *J. Am. Chem. Soc.* **2014**, *136*, 5722–5730.
- (9) Yao, Z.; Zhang, M.; Wu, H.; Yang, L.; Li, R.; Wang, P. Donor/Acceptor Indenoperylene Dye for Highly Efficient Organic Dye-Sensitized Solar Cells. *J. Am. Chem. Soc.* **2015**, *137*, 3799–3802.
- (10) Tan, L. L.; Huang, J. F.; Shen, Y.; Xiao, L. M.; Liu, J. M.; Kuang, D. B.; Su, C. Y. Highly Efficient and Stable Organic Sensitizers with Duplex Starburst Triphenylamine and Carbazole Donors for Liquid and Quasi-Solid-State Dye-Sensitized Solar Cells. *J. Mater. Chem. A* **2014**, *2*, 8988–8994.
- (11) Qi, Q.; Wang, X.; Fan, L.; Zheng, B.; Zeng, W.; Luo, J.; Huang, K. W.; Wang, Q.; Wu, J. N-Annulated Perylene-Based Push-Pull-Type Sensitizers. *Org. Lett.* **2015**, *17*, 724–727.
- (12) Jia, X. W.; Zhang, W. Y.; Lu, X. F.; Wang, Z. S.; Zhou, G. Efficient Quasi-Solid-State Dye-Sensitized Solar Cells Based on Organic Sensitizers Containing Fluorinated Quinoxaline Moiety. *J. Mater. Chem. A* **2014**, *2*, 19515–19525.
- (13) Lin, H.-W.; Wang, Y.-S.; Yang, P.-F.; Wong, K.-T.; Lin, L.-Y.; Lin, F. Photophysical Studies on D- π -A Dye-Sensitized Solar Cells: Effects of π -Bridge and Hexyloxy Side Chains in Donor Moieties. *Org. Electron.* **2013**, *14*, 1037–1044.
- (14) Li, S. R.; Lee, C. P.; Yang, P. F.; Liao, C. W.; Lee, M. M.; Su, W. L.; Li, C. T.; Lin, H. W.; Ho, K. C.; Sun, S. S. Structure-Performance Correlations of Organic Dyes with an Electron-Deficient Diphenylquinoxaline Moiety for Dye-Sensitized Solar Cells. *Chem. - Eur. J.* **2014**, *20*, 10052–10064.
- (15) Wang, Z.; Liang, M.; Wang, L.; Hao, Y.; Wang, C.; Sun, Z.; Xue, S. New Triphenylamine Organic Dyes Containing Dithieno[3,2-*b*:2',3'-*d*]pyrrole (DTP) Units for Iodine-Free Dye-Sensitized Solar Cells. *Chem. Commun.* **2013**, *49*, 5748–5750.
- (16) Zhang, H.; Fan, J.; Iqbal, Z.; Kuang, D.-B.; Wang, L.; Meier, H.; Cao, D. Novel Dithieno[3,2-*b*:2',3'-*d*]pyrrole-Based Organic Dyes with High Molar Extinction Coefficient for Dye-Sensitized Solar Cells. *Org. Electron.* **2013**, *14*, 2071–2081.
- (17) Bai, Y.; Zhang, J.; Zhou, D.; Wang, Y.; Zhang, M.; Wang, P. Engineering Organic Sensitizers for Iodine-Free Dye-Sensitized Solar Cells: Red-Shifted Current Response Concomitant with Attenuated Charge Recombination. *J. Am. Chem. Soc.* **2011**, *133*, 11442–11445.
- (18) Zhang, M.; Wang, Y.; Xu, M.; Ma, W.; Li, R.; Wang, P. Design of High-Efficiency Organic Dyes for Titania Solar Cells Based on the Chromophoric Core of Cyclopentadithiophene-Benzothiadiazole. *Energy Environ. Sci.* **2013**, *6*, 2944–2949.
- (19) Choi, H.; Paek, S.; Lim, K.; Kim, C.; Kang, M.-S.; Song, K.; Ko, J. Molecular Engineering of Organic Sensitizers for Highly Efficient Gel-State Dye-Sensitized Solar Cells. *J. Mater. Chem. A* **2013**, *1*, 8226–8233.
- (20) Lim, K.; Ju, M. J.; Song, J.; Choi, I. T.; Do, K.; Choi, H.; Song, K.; Kim, H. K.; Ko, J. Organic Sensitizers Featuring a Planar Indeno[1,2-*b*]thiophene for Efficient Dye-Sensitized Solar Cells. *ChemSusChem* **2013**, *6*, 1425–1431.
- (21) Wang, X. X.; Guo, L.; Xia, P. F.; Zheng, F.; Wong, M. S.; Zhu, Z. T. Dye-Sensitized Solar Cells Based on Organic Dyes with Naphtho[2,1-*b*:3,4-*b'*]dithiophene as the Conjugated Linker. *J. Mater. Chem. A* **2013**, *1*, 13328–13336.
- (22) Feng, Q.; Jia, X.; Zhou, G.; Wang, Z.-S. Embedding an Electron Donor or Acceptor into Naphtho[2,1-*b*:3,4-*b'*]dithiophene Based Organic Sensitizers for Dye-Sensitized Solar Cells. *Chem. Commun.* **2013**, *49*, 7445–7447.
- (23) Guo, X.; Tsao, H. N.; Gao, P.; Xia, D. B.; An, C. B.; Nazeeruddin, M. K.; Baumgarten, M.; Grätzel, M.; Mullen, K. Dithieno[2,3-*d*:2',3'-*d'*]benzo[1,2-*b*:4,5-*b'*]dithiophene Based Organic Sensitizers for Dye-Sensitized Solar Cells. *RSC Adv.* **2014**, *4*, 54130–54133.
- (24) Wang, Z.; Liang, M.; Tan, Y.; Ouyang, L.; Sun, Z.; Xue, S. Organic Dyes Containing Dithieno [2,3-*d*:2',3'-*d'*]thieno[3,2-*b*:3',2'-*b'*]dipyrrole Core for Efficient Dye-Sensitized Solar Cells. *J. Mater. Chem. A* **2015**, *3*, 4865–4874.
- (25) Eom, Y. K.; Choi, I. T.; Kang, S. H.; Lee, J.; Kim, J.; Ju, M. J.; Kim, H. K. Thieno [3, 2-*b*] [1] benzothiothiophene Derivative as a New π -Bridge Unit in D- π -A Structural Organic Sensitizers with Over 10.47% Efficiency for Dye-Sensitized Solar Cells. *Adv. Energy Mater.* **2015**, *5*, n/a.
- (26) Huang, Z. S.; Feng, H. L.; Zang, X. F.; Iqbal, Z.; Zeng, H. P.; Kuang, D. B.; Wang, L. Y.; Meier, H.; Cao, D. R. Dithienopyrrolo-benzothiadiazole-Based Organic Dyes for Efficient Dye-Sensitized Solar Cells. *J. Mater. Chem. A* **2014**, *2*, 15365–15376.
- (27) Zhou, H.; Yang, L.; Price, S. C.; Knight, K. J.; You, W. Enhanced Photovoltaic Performance of Low-Bandgap Polymers with Deep LUMO Levels. *Angew. Chem., Int. Ed.* **2010**, *49*, 7992–7995.
- (28) Zhou, H.; Yang, L.; Liu, S.; You, W. A Tale of Current and Voltage: Interplay of Band Gap and Energy Levels of Conjugated Polymers in Bulk Heterojunction Solar Cells. *Macromolecules* **2010**, *43*, 10390–10396.
- (29) Yum, J. H.; Hagberg, D. P.; Moon, S. J.; Karlsson, K. M.; Marinado, T.; Sun, L.; Hagfeldt, A.; Nazeeruddin, M. K.; Grätzel, M. A Light-Resistant Organic Sensitizer for Solar-Cell Applications. *Angew. Chem., Int. Ed.* **2009**, *48*, 1576–1580.
- (30) Arroyave, F. A.; Richard, C. A.; Reynolds, J. R. Efficient Synthesis of Benzo [1,2-*b*:6,5-*b'*] dithiophene-4,5-dione (BDTD) and Its Chemical Transformations into Precursors for π -Conjugated Materials. *Org. Lett.* **2012**, *14*, 6138–6141.

- (31) Wang, C.; Liang, M.; Huang, J.; Cheng, F.; Wang, H.; Guo, Y.; Xue, S. Redox Couple Related Influences of Bulky Electron Donor as well as Spacer in Organic Dye-Sensitized Mesoscopic Solar Cells. *Tetrahedron* **2014**, *70*, 6203–6210.
- (32) Link, S. M.; Scheuble, M.; Goll, M.; Muks, E.; Ruff, A.; Hoffmann, A.; Richter, T. V.; Lopez Navarrete, J. T.; Ruiz Delgado, M. C.; Ludwigs, S. Electropolymerized Three-Dimensional Randomly Branched EDOT-Containing Copolymers. *Langmuir* **2013**, *29*, 15463–15473.
- (33) Zhu, W.; Wu, Y.; Wang, S.; Li, W.; Li, X.; Chen, J.; Wang, Z.-S.; Tian, H. Organic D-A- π -A Solar Cell Sensitizers with Improved Stability and Spectral Response. *Adv. Funct. Mater.* **2011**, *21*, 756–763.
- (34) Zhu, H.; Li, W.; Wu, Y.; Liu, B.; Zhu, S.; Li, X.; Ågren, H.; Zhu, W. Insight into Benzothiadiazole Acceptor in D-A- π -A Configuration on Photovoltaic Performances of Dye-Sensitized Solar Cells. *ACS Sustainable Chem. Eng.* **2014**, *2*, 1026–1034.
- (35) Wu, Y.; Marszalek, M.; Zakeeruddin, S. M.; Zhang, Q.; Tian, H.; Grätzel, M.; Zhu, W. High-Conversion-Efficiency Organic Dye-Sensitized Solar Cells: Molecular Engineering on D-A- π -A Featured Organic Indoline Dyes. *Energy Environ. Sci.* **2012**, *5*, 8261–8272.
- (36) Kang, X.; Zhang, J.; O'Neil, D.; Rojas, A. J.; Chen, W.; Szymanski, P.; Marder, S. R.; El-Sayed, M. A. Effect of Molecular Structure Perturbations on the Performance of the D-A- π -A Dye Sensitized Solar Cells. *Chem. Mater.* **2014**, *26*, 4486–4493.
- (37) Feng, Q.; Lu, X.; Zhou, G.; Wang, Z.-S. Synthesis and Photovoltaic Properties of Organic Sensitizers Incorporating a Thieno [3, 4-*c*] pyrrole-4, 6-dione Moiety. *Phys. Chem. Chem. Phys.* **2012**, *14*, 7993–7999.
- (38) Pei, K.; Wu, Y.; Islam, A.; Zhang, Q.; Han, L.; Tian, H.; Zhu, W. Constructing High Efficiency D-A- π -A Featured Solar Cell Sensitizers: a Promising Building Block of 2,3-Diphenylquinoxaline for Anti-aggregation and Photo-stability. *ACS Appl. Mater. Interfaces* **2013**, *5*, 4986–4995.
- (39) Ito, S.; Zakeeruddin, S. M.; Humphry-Baker, R.; Liska, P.; Charvet, R.; Comte, P.; Nazeeruddin, M. K.; Péchy, P.; Takata, M.; Miura, H.; Uchida, S.; Grätzel, M. High-Efficiency Organic-Dye-Sensitized Solar Cells Controlled by Nanocrystalline-TiO₂ Electrode Thickness. *Adv. Mater.* **2006**, *18*, 1202–1205.
- (40) Qian, X.; Zhu, Y. Z.; Chang, W. Y.; Song, J.; Pan, B.; Lu, L.; Gao, H. H.; Zheng, J. Y. Benzo[*a*]carbazole-Based Donor- π -Acceptor Type Organic Dyes for Highly Efficient Dye-Sensitized Solar Cells. *ACS Appl. Mater. Interfaces* **2015**, *7*, 9015–9022.
- (41) Hua, Y.; Chang, S.; He, J.; Zhang, C.; Zhao, J.; Chen, T.; Wong, W. Y.; Wong, W. K.; Zhu, X. Molecular Engineering of Simple Phenothiazine-Based Dyes to Modulate Dye Aggregation, Charge Recombination, and Dye Regeneration in Highly Efficient Dye-Sensitized Solar Cells. *Chem. - Eur. J.* **2014**, *20*, 6300–6308.
- (42) Cui, Y.; Wu, Y.; Lu, X.; Zhang, X.; Zhou, G.; Miapéh, F. B.; Zhu, W.; Wang, Z.-S. Incorporating Benzotriazole Moiety to Construct D-A- π -A Organic Sensitizers for Solar Cells: Significant Enhancement of Open-Circuit Photovoltage with Long Alkyl Group. *Chem. Mater.* **2011**, *23*, 4394–4401.
- (43) Huang, Z. S.; Cai, C.; Zang, X. F.; Iqbal, Z.; Zeng, H. P.; Kuang, D. B.; Wang, L. Y.; Meier, H.; Cao, D. R. Effect of the Linkage Location in Double Branched Organic Dyes on the Photovoltaic Performance of DSSCs. *J. Mater. Chem. A* **2015**, *3*, 1333–1344.
- (44) Zang, X.-F.; Zhang, T.-L.; Huang, Z.-S.; Iqbal, Z.; Kuang, D.-B.; Wang, L.; Meier, H.; Cao, D. Impact of the Position Isomer of the Linkage in the Double D-A Branch-Based Organic Dyes on the Photovoltaic Performance. *Dyes Pigm.* **2014**, *104*, 89–96.
- (45) Li, S. R.; Lee, C. P.; Kuo, H. T.; Ho, K. C.; Sun, S. S. High-Performance Dipolar Organic Dyes with an Electron-Deficient Diphenylquinoxaline Moiety in the π -Conjugation Framework for Dye-Sensitized Solar Cells. *Chem. - Eur. J.* **2012**, *18*, 12085–12095.
- (46) Zang, X.-F.; Huang, Z.-S.; Wu, H.-L.; Iqbal, Z.; Wang, L.; Meier, H.; Cao, D. Molecular Design of the Diketopyrrolopyrrole-Based Dyes with Varied Donor Units for Efficient Dye-Sensitized Solar Cells. *J. Power Sources* **2014**, *271*, 455–464.
- (47) Li, Q.; Shi, J.; Li, H.; Li, S.; Zhong, C.; Guo, F.; Peng, M.; Hua, J.; Qin, J.; Li, Z. Novel Pyrrole-Based Dyes for Dye-Sensitized Solar Cells: From Rod-Shape to "H" Type. *J. Mater. Chem.* **2012**, *22*, 6689–6696.
- (48) Zhang, W.; Feng, Q.; Wang, Z. S.; Zhou, G. Novel Thiazolo[5,4-*d*]thiazole-Based Organic Dyes for Quasi-Solid-State Dye-Sensitized Solar Cells. *Chem. - Asian J.* **2013**, *8*, 939–946.
- (49) Cai, S.; Hu, X.; Zhang, Z.; Su, J.; Li, X.; Islam, A.; Han, L.; Tian, H. Rigid Triarylamine-Based Efficient DSSC Sensitizers with High Molar Extinction Coefficients. *J. Mater. Chem. A* **2013**, *1*, 4763–4772.
- (50) Wang, L.; Yang, X.; Zhao, J.; Zhang, F.; Wang, X.; Sun, L. Efficient Organic Sensitizers with Pyridine-N-oxide as an Anchor Group for Dye-Sensitized Solar Cells. *ChemSusChem* **2014**, *7*, 2640–2646.
- (51) Cheng, M.; Yang, X.; Li, J.; Chen, C.; Zhao, J.; Wang, Y.; Sun, L. Dye-Sensitized Solar Cells Based on a Donor-Acceptor System with a Pyridine Cation as an Electron-Withdrawing Anchoring Group. *Chem. - Eur. J.* **2012**, *18*, 16196–16202.
- (52) Tan, H.; Pan, C.; Wang, G.; Wu, Y.; Zhang, Y.; Zou, Y.; Yu, G.; Zhang, M. Phenoxazine-Based Organic Dyes with Different Chromophores for Dye-Sensitized Solar Cells. *Org. Electron.* **2013**, *14*, 2795–2801.